Doctoral Thesis

Novel transgenic enteroid to establish platform for investigating mechanisms of intestinal epithelial cell function

(新規遺伝子改変 enteroid を用いた小腸上皮細胞機能解析プラットフォームの開発)

Shuya OHIRA

Innate Immunity Laboratory

Transdisciplinary Life Science Course

Graduate school of Life Science

Hokkaido University

2023.3

Contents

1. Introduction

Intestine is continually exposed to food-derived substances and pathogens intaken to the intestinal lumen, in addition to commensal bacteria that shape intestinal microbiota. Epithelial cells in the small intestine form a single layer that divides the external environment inside the lumen from the subepithelial tissue. Small intestine elicit important functions such as nutrient absorption, metabolism, and immunity to contribute to maintaining life and its homeostasis[1,2]. Small intestinal epithelial cells consists of the absorptive cell responsible for nutrient absorption in the villus, the enteroendocrine cell associated with digestion and metabolism, the goblet cell responsible for barrier by mucus secretion, and the Paneth cell at the base of the crypt which contributes to innate immunity by secreting granules rich in antimicrobial peptides largely α-defensins[3–5]. All these terminally differentiated cells are provided by self-renewal and differentiation of the intestinal epithelial stem cells (IESCs) localized at the crypt base[6]. Furthermore, it has been known that IESCs and Paneth cells which reside adjacent to the IESCs constitute stem cell niche for the small intestinal epithelia[7]. However, molecular mechanisms underlying functions of the small intestinal epithelial cells, including their effects against the external environment in the lumen and internal environment in the subepithelial tissue, remain unknown.

Two-dimensional cultured cancer-derived intestinal epithelial cell lines have been widely used for aiming to analyze the molecular mechanisms of function by the intestinal epithelial cells,

though, there are problems that these cell lines are not always reflecting normal intestinal epithelial cell function *in vivo*[8,9]. On the other hand, small intestinal epithelial organoid named enteroid was established. The enteroid is a three-dimensional culture system enabling to culture for a long term that mimics *in vivo* small intestinal epithelial structure, constructing the villus and crypt-like structures composed of IESCs and all terminally differentiated epithelial cells[10]. To date, enteroids have been made from normal or disease model mice having physiological or pathophysiological functions and analyzed for mechanisms in normal and in pathophysiology including nutrient absorption, drug transport, hormone secretion, innate immunity, regeneration, and differentiation[11–13]. In the enteroid analyses, biochemical approaches using ligands, inhibitors, and probes have been generally used. These biochemical methods are known to be characteristically dependent on conditions such as concentration in the binding and inhibitory activity or selectivity, and these factors sometimes crucially influence especially on 3D structure-formed cell samples including enteroids. Therefore, a genetic approach to the enteroid advantageous to controlling target expression specifically, named transgenic enteroid has been developed. Transgenic enteroids are produced from cultured enteroids in extracellular matrix gels or intact isolated crypts, both separated into single cells, followed by accessing expression vector to single IESCs[14–16]. However, there are limitations in the conventional transgenic enteroid producing method such as low gene transfer efficiency, complexity, and cytotoxicity due to necessary preparation of chemical isolation, and time-consuming because of

producing enteroid from a single IESC without stem cell niche maintained. High-efficient gene transfer is known to be achieved by high target cell proportion and viability[17], further reported that IESCs exist only at the base of the crypt-like structure of the enteroid, and their viability is enhanced by stem cell niche signals from adjacent Paneth cells[6,7,10]. Additionally, the method of comprehensive analysis for exploring functional genes of each terminally differentiated cell in small intestinal epithelial cells has not been established[18]. Therefore, we aim to develop a platform for investigating small intestinal epithelial cell function by establishing a highly efficient, quick, and simple method of generating transgenic enteroids and in addition to a method of exploring functional genes followed by sorting.

Here we show that the gene were transferred into intact small intestinal crypts, which possess high proportion and viability of IESCs by keeping intact stem cell niche without separating into single cells, using lentiviral vector to induce stable transgene expression. Olfm4^{+} IESCs were transduced, continued stable expression of the transgene, and formed villus-crypt structures constructed by gene-transferred all lineages of terminally differentiated epithelial cell. It is further shown that P-glycoprotein-mediated drug transport of the small intestinal epithelial cells including absorptive cells and secretion of antimicrobial peptides by Paneth cells in innate immunity in the transgenic enteroids were equivalent to those from intact enteroids. It is also demonstrated that Zinpyr-1 (ZP1)$^{+}$ Paneth cells were enriched by fluorescence activated cell sorting (FACS), and Paneth cells expressed

functional genes of pattern recognition, membrane trafficking, and membrane fusion for innate immunity. Taken together, this study established the novel platform to reveal molecular mechanisms of small intestinal epithelial cell functions through high-throughput analysis based on efficient, simple, and quick transgenic enteroid generation method, which exploits traditional advantages of conventional transgenic enteroids, and functional gene exploration method.

2. Methods

2.1. Mice

C57BL/6 adult male mice and Crl:CD1 (ICR) adult male mice were obtained from CLEA Japan. All animal experiments were approved by the National University Corporation Hokkaido University Animal Experimentation Committee. All experiments were conducted in accordance with relevant guidelines and regulations of Hokkaido University.

2.2. Culture of transgenic enteroid

Small intestinal crypts were isolated as described previously[19,20]. Briefly, C57BL/6 mouse jejunum was rotated in 30 mM EDTA with Ca2+- and Mg2+-free Hank's balanced salt solution (HBSS) for 10 min at room temperature (RT) at 10 rpm. The tissue was vigorously shaken in ice-cold HBSS to exfoliate crypts. The fraction with >80% purity of crypts was used in this study.

To transfer gene, isolated crypts were incubated with rLV-EF1α-tdTomato-IRES-Puro-WPRE

constitutive lentiviral vectors (Takara Bio) in complete medium (CM) including growth factors (EGF, R-Spondin 1, Noggin)[19] with 3 μM CHIR99021 (Miltenyi Biotec) in 48-well plates (Thermo Fisher Scientific) by centrifugation at 600 g for 1 h at 30℃, followed by incubating for 6 h at 37℃, 5% CO_2. Sham crypts were carried out the gene transfer manipulation at the same condition without lentiviral vectors. Intact crypts were performed without the gene transfer manipulation. To examine the effect of polybrene, 10 μg/mL polybrene (nacalai tesque) was added to CM with lentiviral vector and CHIR99021 at the gene transfer manipulation.

To culture enteroid, infected, sham, and intact crypts mixed with 30 μL Matrigel (Corning) were plated in 48-well plates at 150 crypts/well, respectively. After polymerization of Matrigel, CM with (transgenic enteroid, sham enteroid) or without (intact enteroid) 3 μM CHIR99021 was added at 250 μL/well (Figure 1A). After day 2 of culture, the medium was exchanged with 2 μg/mL puromycin in CM (transgenic enteroid) or CM only (intact and sham enteroid) every other day. To assess drug selection condition, intact enteroids were cultured in the presence of 2 μg/mL puromycin after day 2. To passage, transgenic enteroids were mechanically dissociated into crypt-like domains by pipetting and embedded in Matrigel on 48-well plates with a 1:1–2 split ratio. CM with 2 μg/mL puromycin was added and exchanged every other day. The culture was passaged every 7–9 days.

2.3. Quantification of transgene expression in enteroids and enteroid formation

Z-stack images of transgenic enteroids were obtained with 20 μm Z-step using a confocal microscope (A1, Nikon) equipped with 0.13 NA objective lens (Plan Fluor 4X, Nikon). During live cell imaging, enteroids were set at 37°C, 5% CO_2 by using Stage Top Incubator (Tokai Hit). To quantify tdTomato$^+$ area ratio, tdTomato$^+$ area and total enteroid area were measured using the maximum intensity projection images generated from Z-stack images by NIS-Elements AR (Nikon), and the percentage of tdTomato$^+$ area in total enteroid area was calculated as tdTomato$^+$ area ratio. To quantify tdTomato intensity, enteroid images of primary culture at day 7 and passaged culture at day 4 or 5 were obtained by a confocal microscope with 0.13 NA objective lens and tdTomato intensity in epithelial cells of enteroids was measured by NIS-Elements.

To quantify transgenic enteroid yield, enteroid number was counted under an inverted routine microscope (Eclipse Ts2, Nikon), and transgenic enteroid yield was calculated as the percentage of transgenic enteroid number to sham enteroid number. To quantify enteroid formation, number of seeded crypts at day 0 and enteroids at each day was counted under inverted routine microscope, and enteroid forming efficiency was calculated as the percentage of enteroid number to crypt number.

2.4. Immunofluorescence staining

Enteroids were immunostained as described previously[19]. Briefly, enteroids were fixed with 4% paraformaldehyde (Sigma-Aldrich), followed by permeabilizing and blocking with 0.1% Triton X-100

(Sigma-Aldrich) and 5% goat serum (Sigma-Aldrich). Primary antibody reaction was performed by using 12 μg/mL rabbit anti-Olfm4 (clone: D6Y5A, Cell Signaling) and 5 μg/mL rat anti-Ki-67 (clone: SolA15, Invitrogen), or rabbit anti-Villin (dilution 1:100, clone: SP145, Abcam), or 1 μg/mL rabbit anti-Muc2 (Santa Cruz Biotechnology), or rabbit anti-Chromogranin A (ChgA, dilution 1:500, ImmunoStar), or 10 μg/mL rat anti-α-defensin (clone: 77-R63)[21]. Secondary antibody reaction was performed by using Alexa Fluor 488 goat anti-Rat IgG antibody and Alexa Fluor 647 goat anti-Rabbit IgG, or Alexa Fluor 488 goat anti-Rabbit IgG (dilution 1:400, Thermo Fisher Scientific). Enteroids were also stained with 5 μg/mL 4', 6-diamidino-2-phenylindole (DAPI, Thermo Fisher Scientific) for 5 min at RT and mounted with RapiClear 1.52 (Sunjin Lab). Stained enteroid images were taken using a confocal microscope with 0.95 NA objective lens (CFI Apo LWD 20x WI λS, Nikon).

To quantify transduction efficiency, the number of $tdTomato^{+}Olfm4^{+}$ cells and total $Olfm4^{+}$ cells in 37–61 enteroids were counted. Transduction efficiency was calculated as the percentage of $tdTomato^{+}$ cell number in total cell number.

To quantify terminally differentiated cell ratio, the number of marker-expressing cells and total cells in enteroids were counted by NIS-Elements AR, and terminally differentiated cell ratio was calculated as the percentage of marker-expressing cell number in total cell number.

2.5. Quantification of drug transport

Enteroids were separated from Matrigel with ice-cold Advanced DMEM/F12 and transferred onto collagen-coated 8 well chamber cover (Matsunami) at 100 enteroids/well. The chamber was placed on ice for 5 min to sink enteroids to the bottom. Matrigel was polymerized followed by adding CM pre-warmed to 37ºC. Chamber was fixed on Stage Top Incubator at 37ºC, 5%CO_2. Three enteroids were followed up 0, 5, 15, 30, 60, 120, and 180 min after adding 1 μM Rh123 (Sigma-Aldrich) in CM by a confocal microscope with 0.95 NA objective lens. Rh123 intensity inside the enteroid lumen was measured by NIS-Elements AR.

2.6. Quantification of Paneth cell granule secretion

Visualization and quantification of Paneth cell granule secretion were conducted as described previously[19]. Briefly, enteroids on the 8 well chamber cover were stimulated with 1 μM CCh for 30 min at 37ºC, 5%CO_2, and time-lapse imaging was conducted using a confocal microscope with 0.95 NA objective lens. Percent granule secretion was calculated based on Paneth cell granule area at pre- and post-stimulation measured by NIS-Elements AR.

2.7. Fluorescence activated cell sorting

FACS was conducted as described previously[20]. Briefly, crypts were collected from whole small intestine of ICR mice. Isolated crypts were dissociated by shaking at 180 rpm in HBSS containing 300

U/mL collagenase (Sigma-Aldrich), 10 μM Y-27632 (Sigma-Aldrich), and 1 mM N-acetylcysteine (Sigma-Aldrich) for 10 min at 37°C on a horizontal shaker (TAITEC), followed by pipetting with 50 μg/mL DNaseI (Roche). Dissociated cells were passed through 40 μm cell strainer (Corning) and stained by 10 μM Zinpyr-1 (ZP1, Santa Cruz) for 15 min at 37°C. $ZP1^+$ cells were sorted as Paneth cell using a cell sorter (JSAN, Bay Bioscience). Doublets were excluded by gating on forward scatter height vs forward scatter area (Figure 11). Cell images before and after sorting were acquired under an inverted routine microscope (CKX31, Olympus).

2.8 RNA-Sequencing analysis

For RNA-Sequencing (RNA-seq) analysis of Paneth cells, 200−33,000 Paneth cells were sorted from 1 mouse, and pooled sample was made from 10 mice. Total RNA was isolated using Invitrogen® PureLink RNA Purification System according to manufacturer's instructions. Library preparation and sequencing by Illumina HiSeq for 100-bp PE reads were outsourced to APRO Science. Fragment per kilobase of transcript per million mapped reads (FPKM) values were used and genes with FPKM values below 1 were not included in the analysis.

2.8. Statistical analysis

Statistical significance was determined using two-tailed unpaired Student's t-test, one-way ANOVA

with multiple comparison's test (Tukey's, Dunnett's), and two-way analysis of variance (ANOVA) with Bonferroni's multiple comparison's test as indicated in figure legends by using GraphPad Prism ver. 9.0 software (GraphPad Software). $P < 0.05$ was considered statistically significant.

3. Results

3.1. Establishment of a highly efficient, quick, and simple method for transgenic enteroid production

3.1.1 Transgenic enteroids are generated by gene transfer into isolated crypts

First, to establish transgenic enteroids by gene transfer into intact isolated crypts, mouse isolated crypts were introduced 5.0×10^3 transduction units (TU)/crypt of lentiviral vector expressing tdTomato and puromycin resistant gene, and three-dimensional culture followed by drug selection and observation with confocal microscopy over time were conducted (Figure 1A). Polybrene is often used to enhance gene transfer efficiency[22], though, it was not used because almost all enteroids disrupted within 5 days after adding it (Figure 2). Next, to determine concentration of puromycin and period of treatment for the drug selection, non-transfected enteroids, i.e., intact enteroids were treated with 2 μg/mL puromycin from day 2, and all enteroids died at day 7 (Figure 3), indicating that drug selection was completed by day 7 under the condition. Gene-transferred isolated crypts constructed enteroids from day 1, and tdTomato expression was first observed at the base of crypt-like structures at day 2 (Figure 1B and 4). Then, transgenic enteroids composed only of $tdTomato^+$ cells were observed at day 7. In addition, from day 7 to 9, tdTomato continued expressing, crypt-like structures continued to elongate, and transgenic enteroids were not disrupted. When evaluation of transgenic enteroid forming process was conducted by quantifying the ratio of the $tdTomato^+$ area in total area of enteroids, the

tdTomato^{+} area ratio was 50.3 ± 2.68, 66.7 ± 4.84, and 94.2 ± 1.97% at day 2, 3, and 5, respectively, and tdTomato were expressed in all cells at day 7 and after (Figure 1C). Furthermore, the yield of transgenic enteroid calculated was 56 ± 7.4 and 62 ± 7.4% at day 7 and 9, respectively (Figure 1D). The efficiency of enteroid formation between presence and absence of gene transduction showed no difference (Figure 5). Thus, transgenic enteroids were obtained with high efficiency by day 7.

To confirm whether the transgenic enteroid generated by this gene transfer method keeps expression of the transgene over time, transgenic enteroids introduced tdTomato were passaged three times and cultured for one month. The tdTomato intensity measured at passage 0, 1, 2, and 3 was 1601 ± 70, 1299 ± 60, 1548 ± 74, and 1372 ± 112 arbitrary units (AU), respectively. Fluorescence intensity at each passage culture was not different compared that at primary culture (Figure 6), indicating that transgene expression maintains in these passages.

Furthermore, to determine the titer of lentiviral vector required for generating transgenic enteroids, transgenic enteroids were produced with different titers, 5.0×10^{3}, 5.0×10^{2}, or 5.0×10 TU/crypt of lentiviral vector, harvested at day 7, and the yield of transgenic enteroid was calculated. The yield was 57 ± 3.7 and 54 ± 11% on 5.0×10^{3} and 5.0×10^{2} TU/crypt, respectively, showing no difference. On the other hand, the yield was 18 ± 7.7% on 5.0×10 TU/crypt, showing significant decrease compared to both 5.0×10^{3} and 5.0×10^{2} TU/crypt (Figure 7).

3.1.2. Intestinal epithelial stem cells in the transgenic enteroids are gene transferred

To assess the efficiency of target gene transfer into IESCs, we examined Olfm4, which is expressed specifically in IESCs[23]. Immunofluorescence staining was performed on day 2 enteroids, which started to express tdTomato, and tdTomato$^+$ cells in Olfm4$^+$ IESCs were 25 ± 2.1% (Figure 8). These results indicated that the gene transfer into IESCs is elicited by lentiviral infection to isolated crypts.

3.2 Evaluation for intestinal functions of the transgenic enteroid

3.2.1 Transgenic intestinal epithelial stem cells maintain multipotency

Next, to evaluate whether the transgenic IESCs maintain their ability to differentiate into all lineages of terminally differentiated cells, immunofluorescence staining of molecules expressed specifically in absorptive cells, goblet cells, enteroendocrine cells, and Paneth cells was conducted on day 7 transgenic enteroids. Epithelial cells that constitute enteroids exhibit apical-basal polarity with apical on the inner (lumen) side and basal on the outer side of the enteroids[10,19]. The transgenic enteroids possessed tdTomato$^+$ absorptive cells with villin expression on the apical side of villus-like structures (Figure 9A). The tdTomato$^+$ goblet cells (Muc2$^+$, Figure 9B) and tdTomato$^+$ enteroendocrine cells (ChgA$^+$, Figure 9C) were scattered on the villus- and crypt-like structures of the transgenic

enteroids. In addition, the transgenic enteroids had tdTomato$^+$ Paneth cells at the base of crypt-like structures with apical α-defensin expression (Figure 9D). The percentage of each maker expressing cells in the intact and transgenic enteroids was 51.3 ± 6.3 and 42.6 ± 7.4% in villin$^+$ cells (Figure 9E), 8.0 ± 1.4 and 7.2 ± 1.1% in Muc2$^+$ cells (Figure 9F), 1.4 ± 0.3 and 2.1 ± 0.3% in ChgA$^+$ cells (Figure 9G), and 6.6 ± 1.1 and 6.3 ± 1.0% in α-defensin$^+$ cells (Figure 9H), respectively, showing no difference. These results indicated that the transgenic IESCs maintain their multipotency to differentiate into all lineages of terminally differentiated epithelial cells in the small intestine with keeping polarity and construct intact villus- and crypt-like structures.

3.2.2 Terminally differentiated cells from transgenic intestinal epithelial stem cells maintain intestinal functions

Because intestinal epithelial cell functions are roughly divided into the absorption and the secretion[3], the drug transport ability largely of absorptive cells and the granule secretion ability of Paneth cells on day 7 intact and transgenic enteroids were examined to evaluate whether the terminally differentiated cells derived from transgenic IESCs elicit intact intestinal function. Rhodamine 123 (Rh123) intensities in the intact and transgenic enteroid lumen were measured at 0, 5, 15, 30, 60, 120, and 180 minutes after adding Rh123 to the culture medium, and 243.08 ± 0.40, 247.88 ± 2.51, 262.41 ± 4.12, 303.68±6.92, 372.81 ± 5.97, 476.33 ± 26.67, and 495.34 ± 37.53 AU in intact enteroids,

respectively, and 244.03 ± 0.96, 245.13 ± 1.25, 250.48 ± 2.96, 274.52 ± 9.16, 336.77 ± 18.84, 506.97 ± 72.25, and 570.96 ± 74.03 AU in transgenic enteroids (Figure 10A and B), showing no difference at each time. When CCh was added to the medium of the intact and transgenic enteroids, tdTomato^{+} Paneth cells intensely secreted granules within 30 minutes after addition of CCh, similar to intact Paneth cells (Figure 10C). The granule secretion rate of Paneth cells calculated at 30 minutes after adding CCh in the intact and transgenic enteroids was 75.1 ± 3.61 and 83.1 ± 4.02%, respectively, and showed no difference (Figure 10D), indicating that the process of gene transfer does not affect the Paneth cell secretory function. These results indicated that absorptive cells and Paneth cells differentiated from transgenic IESCs exhibit intact function.

3.3 Exploration of functional genes by sorting intestinal epithelial cells and RNA-sequencing

3.3.1 Paneth cells are enriched by sorting

Since it is reported that Paneth cells secrete granules containing α-defensin exocytotically[19,24] in response to food, bacterial antigens, and cholinergic stimuli for innate enteric immunity and regulation of intestinal microbiota[1,4], focused on mechanisms of Paneth cell function from recognition of internal and external environment to granule secretory response. First, to enrich Paneth cells for exploration of the possible functional genes, FACS was conducted using ZP1, probe

of zinc specifically appeared in Paneth cell granules in the small intestinal epithelial cells[25]. Paneth cells were greatly enriched by sorting $ZP1^+$ singlet cells and purity of Paneth cells after sorting was 93.0±1.3%. These results indicated that highly Paneth cell-rich pool is obtained by FACS.

3.3.2 Candidates of functional genes associated with Paneth cell granule secretion are identified by RNA-sequencing

Finally, to determine functional genes of Paneth cell, RNA-Seq analysis of enriched Paneth cells was conducted, and total 8973 genes were detected. To identify target genes for receptors by which Paneth cells recognize surrounding intestinal environment, genes annotated with gene ontology (GO) term "transmembrane signaling receptor activity" were explored. Paneth cells expressed 120 genes annotated with "transmembrane signaling receptor activity" including *P2rx4*, *Tlr5*, *Fgfrl1*, and *IL22ra1*. Furthermore, to identify target genes inducing Paneth cell granule secretion after recognition, genes annotated with GO term "exocytosis" were explored. Paneth cells expressed 105 genes annotated with "exocytosis" including *Rab3d*, *Tmed10*, *Vamp8*, and *Napa*. These results demonstrated that the platform with enriching certain small intestinal epithelial cells enables to identify candidates of functional genes in Paneth cells for instance, and Paneth cells express these functional genes in association with the granule secretory function.

4. Discussion

4.1 Efficiency, quickness, and simplicity of the established transgenic enteroid generation method

Aiming at investigation of small intestinal epithelial cell function, a transgenic enteroid that expresses a target gene using viral vector has been developed and used. In conventional method for producing transgenic enteroids from single cells, which needs single-cell preparation, there were potential problems of low generation efficiency in the complicated, time-consuming processes[14–16].

This study demonstrated that by transferring a gene into IESCs without separating intact small intestinal crypts, transgenic enteroids in which all cells expressed the transgene were generated with yield of 56%. The small intestinal epithelial tissue *in vivo* is reported to possess about 500 cells in villi, and 250 cells in crypts containing approximately 15 cells of IESCs[26–28]. Transgenic enteroids have been acquired previously from single cells separated from enteroids[14,15] or isolated small intestinal crypts[16]. Schwank et al. generated transgenic enteroids by electroporation of single cells separated from enteroids, and the yield is estimated as 9% based on the above *in vivo* condition[15]. Onuma et al. produced transgenic enteroids by lentiviral transduction of single cells separated from isolated small intestinal crypts, and the yield is estimated as 20%[16]. It has been known that IESCs which provide all terminally differentiated epithelial cells are supported by neighboring Paneth cells

providing niche signals[7], so that IESCs and Paneth cells form stem cell niche. Thus, the novel gene transfer method we established using intact isolated small intestinal crypts is suggested to elicit high yield of transgenic enteroids, because of effective transfer of the target gene into IESCs by using intact isolated crypts maintaining stem cell niche that is formed by the stem cell and adjacent Paneth cell, as well as high IESC viability.

This study demonstrated that transgenic enteroids are acquired as early as in a week by using isolated crypts without chemical dissociation. Previously, it took at least 2 to 3 weeks to obtain transgenic enteroids by using single cells that were physically separated from 3-dimensional cultured enteroids[14,15,29]. Additionally, the gene transfer into chemically separated single cells from isolated crypts was reported to take about 10 days[16]. Because no additional enteroid culture and chemical dissociation to single cells prior to gene transfer are needed, gene transfer method in this study is not only simple but also quicker than those conventional methods. Moreover, transgenic enteroids were even produced with the lentiviral vector titer as low as 5.0 × 10 TU/crypt. The lentiviral vector titer in the packaging cell line culture supernatant is reported in the range of 1×10^5–10^7 TU/mL when made at a bench scale[30–32]. Since concentration of lentiviral vector is not needed, the novel method further enables to generate transgenic enteroids more easily and cost-effectively. Taken together, transgenic enteroid production method in this study has clear advantages compared to conventional methods.

Transgene expression in transgenic enteroids generated by conventional methods using viral

vectors has been reported to last for 3–5 weeks[14,16]. The transgenic enteroid generated by the novel gene transfer system keeps expressing the transgene through passages as in the conventional methods so that it enables repeating and high-throughput analyses without preparing from isolated crypts each time.

4.2 Application of the transgenic enteroid for investigating intestinal epithelial cell function

Because enteroid reflects functions of intestinal epithelial cells more accurately compared to 2-dimensional cultures such as cancer-derived intestinal epithelial cell lines[8–10], enteroids are widely used for analyzing intestinal functions including nutrient absorption[33], drug transport[34], endocrine[35], innate immunity[11,19,24,36], regeneration, and differentiation[7,20]. Furthermore, enteroids generated from disease model animals contribute to understanding the pathophysiology of diseases[37,38] and drug screening aimed to discover drugs[13,39]. Although biochemical methods using such as ligands, inhibitors, and probes and biological methods including using antibodies are often used to examine molecular mechanisms of the intestinal epithelial cell functions in enteroids, these methods greatly depend on experimental conditions such as the selectivity and intensity of these activities. Thus, transgenic enteroids, which specifically regulate target expression, have been developed by gene transfer using vectors such as retroviruses and lentiviruses, and analyzed[12,14].

Previously it is reported that retroviral and lentiviral vectors carry the risk of causing

insertional mutation through the integration of transgenes into host genome using hematopoietic stem cells, though, the genotoxicity of lentiviral vector is lower than that of retroviral vector[40,41]. There has been no report to analyze effects of gene transfer on the function of terminally differentiated intestinal epithelial cells using transgenic enteroids generated with viral vectors, except for limited reports discussing proliferation and differentiation of IESCs[14,29]. Transgenic enteroids with small intestinal epithelial structure consisting of all terminally differentiated cells were formed by IESCs in intact isolated crypts transfected with lentiviral vector, and the transgenic enteroids retained ability of drug-transport in mainly absorptive cells and granule secretion in Paneth cells. In addition, extra reagents are needed to add to culture medium when enteroids are made from single cells without stem cell niche[42,43]. The reagents including CHIR99021, a GSK3β inhibitor, and nicotinamide[44], a selective inhibitor of multiple kinases such as ROCK and Sirtuins, inhibit differentiation of stem cells to terminally differentiated cells[42], suggesting that their use results in loss of *in vivo* function in enteroids. In contrast, our method to generate transgenic enteroids from niche-maintaining isolated crypts does not affect the intestinal function because those reagents are not needed. Therefore, the established method is not only more suitable for the analysis of intestinal function, but also more efficient, quicker, and cost-effective compared to conventional transgenic enteroids. It is applicable for uncovering molecular mechanisms of intestinal function, which are difficult to observe *in vivo* and real-time, and expected to contribute to the development of functional foods and drug discovery.

4.3 The functional gene exploration method for investigating intestinal epithelial cell function in the platform

For functional analysis using the transgenic enteroid, target genes, candidates for functional genes, are needed to be selected. Functional genes expressed in terminally differentiated small intestinal epithelial cells have been explored using single cell RNA-seq (scRNA-seq)[18], though, there are limitations including low sensitivity in genes with low abundance[45]. The comprehensive genetic analysis of the terminally differentiated cells was also limited because of difficulties in enriching each terminally differentiated cell[7]. This study showed that Paneth cells, one lineage of small intestinal epithelial cells, were isolated with high purity by FACS analysis using probe for zinc to explore functional genes. Previously, antibodies against CD24 were used for Paneth cell isolation[7,46], though, IESCs also express CD24[47], so that it has been difficult to isolate Paneth cells with high purity. It is reported that zinc appears specifically in Paneth cell granules in small intestinal epithelial cells[25], and the ZP1 was previously used for observing Paneth cell degranulation[48]. Further, our laboratory reported that Paneth cells isolated by ZP1 express receptor genes for food-derived substances[24], genes associated with innate immunity[49], cytokine receptor[21], and also reported comprehensive gene expression in subsets of $ZP1^{+}$ Paneth cells[36], though, purity of Paneth cells were not reported yet. This study demonstrated that Paneth cells are enriched with 93% purity suitable for identifying candidates

of functional genes. In addition, the previous report detects up to 1600 genes with 3' droplet based scRNA-seq and up to 6000 genes with full length scRNA-seq of small intestinal epithelial cells[18]. This study detected 8973 genes by RNA-seq of enriched Paneth cells, indicating that our functional gene exploration method is highly sensitive and effective to identify target genes with low abundance.

Among small intestinal epithelial cells, Paneth cells secrete granules rich in antimicrobial peptide mainly α-defensins in the innate enteric immunity[4,50] and regulate the intestinal microbiota[1,51,52] for systemic homeostasis. Furthermore, it is reported that decrease of intact α-defensin secretion or secretion of abnormal reduced-form α-defensin by Paneth cells contributes to the pathophysiology of graft-versus-host disease[49,53,54], inflammatory bowel disease[37,55] and depression[56] via disruption of the intestinal microbiota. About mechanisms of Paneth cell granule secretion, Paneth cells are presented to respond to the amino acid leucine via Slc7a8[24], the short-chain fatty acid butyrate via Gpr41[24], the pathogenic bacteria *S.* Typhimurium and its bacterial component LPS[19], and cholinergic stimuli CCh, etc. However, the molecular mechanisms of Paneth cell function from the recognition of the external environment, including a wide variety of food components, bacterial components, and bacterial metabolites, as well as the internal environments created by the host cell, to the secretory response are mostly unknown. In this study, RNA-seq analysis with enriched Paneth cells identified 120 genes annotated with the GO term "transmembrane signaling activity" including *P2rx4*, *Tlr5*, *Fgfrl1* and *IL22ra1*. Our results also showed that 105 genes annotated with

"exocytosis" including *Rab3d*, *Tmed10*, *Vamp8*, and *Napa* were identified in Paneth cells. Purinergic receptor P2X4 (P2rx4), a pattern recognition receptor (PRR) for damage associated molecular patterns (DAMPs), induces brain-derived neurotrophic factor secretion in microglia causing neuropathic pain, and induces mucus secretion for barrier function in goblet cells of lung epithelium, and the induction in both cases are via intracellular calcium influx in response to extracellular ATP. In Paneth cells, increased intracellular calcium levels induce granule secretion[4,19,57], so that strongly suggested that Paneth cells recognize extracellular ATP by P2rx4 to secrete granules. Toll like receptor 5 (TLR5)[58], one of the PRRs for pathogen associated molecular patterns (PAMPs), induces MMP-9-containing granule secretion by neutrophils[59] and Myd88-mediated mucus secretion by colonic goblet cells[60,61]. Paneth cells are reported to express mRNAs for several toll like receptors including TLR5 by nested PCR of isolated Paneth cells[62], suggesting TLR5-mediated Paneth cell granule secretion in response to bacterial components. Fibroblast growth factor receptor like 1 (FGFRL1) is found in pancreatic β-cell membranes and insulin-containing secretory granules and promotes ERK1/2[63], a MAPK, that induces insulin secretion by glucose[64], suggesting that Paneth cells granule secretion associates with recognition of host-derived cytokines via Fgfrl1. IL-22 receptor subunit α1 (IL22ra1) associated with host defense[65] and colitis[66] in the intestinal tract. Previous study showed that IL-22 increases expression of antimicrobial peptide and protein[67] and α-defensin secretion[36] in Paneth cells, suggesting its involvement in Paneth cell granule secretion. Thus, in the platform which is developed

in this study, candidates of target genes in PRRs for DAMPs and PAMPs, and cytokine receptors involved in Paneth cell function were identified.

Rab proteins are monomeric GTPases and known to be responsible for vesicular trafficking from vesicle formation to plasma membrane via the Golgi apparatus[68]. In particular, Rab3d induces IgE receptor-mediated secretion of histamine-containing granules in mast cells[69] and amylase-containing granules by pancreatic acinar cells[70]. Also, it has also been reported that Paneth cells express mRNA for several Rab proteins[36], though, how they are involved in secretion is completely unknown. Furthermore, p24 family proteins are also involved in vesicular trafficking from the endoplasmic reticulum to the Golgi apparatus, associated with insulin secretion by pancreatic β-cells[71]. Among them, transmembrane P24 trafficking protein 10 (Tmed10) transports cytoplasmic proteins into the Golgi apparatus to form secretory granules[72], though it is largely unknown how and in which cells, Tmed10 is involved in granule secretion. Vamp8 is reported to form a soluble N-ethylmaleimide-sensitive factor attachment protein receptor (SNARE), which induces granule secretion in pancreatic acinar cells[73] and mucin secretion by goblet cells in the airways[74]. In addition, N-ethylmaleimide-sensitive factor attachment protein α (α-SNAP) is reported to form SNARE[75] and induce catecholamine-containing granule secretion by chromaffin cells in the adrenal medulla[76]. Therefore, candidates of target genes for vesicular trafficking and membrane fusion-related proteins such as Rab proteins, p24 family proteins, and SNARE proteins involved in Paneth cell function were identified in

the novel platform.

Taken together, this study showed that Paneth cells were enriched with high purity from mixture in several lineages of small intestinal epithelial cells, enabling to identify candidates of functional genes in Paneth cells, suggesting that the platform is useful in high throughput exploring for functional genes of intestinal epithelial cells.

5. Conclusion

This study develops a novel platform for investigating intestinal epithelial cell function by establishing transgenic enteroids production method that is more efficient, easier, and quicker than the conventional method by transferring genes into isolated small intestinal crypts without single cell separation, and exploration method of candidate genes by RNA-Seq using intestinal epithelial cells sorted with high purity. In this platform, transgenic enteroids maintain their intact functions of the absorptive and secretory intestinal epithelial cells indicating suitable for functional analyses, and candidates of functional genes in Paneth cells are identified. This study contributes to elucidation of molecular mechanism for small intestinal epithelial cells in maintaining homeostasis through high-throughput analysis.

6. References

1. Nakamura, K., Sakuragi, N., Takakuwa, A. & Ayabe, T. Paneth cell α-defensins and enteric microbiota in health and disease. *Biosci Microbiota Food Health* **35**, 57–67 (2016).

2. Kurashima, Y. & Kiyono, H. Mucosal Ecological Network of Epithelium and Immune Cells for Gut Homeostasis and Tissue Healing. *Annu. Rev. Immunol.* **35**, 119–147 (2017).

3. Beumer, J. & Clevers, H. Cell fate specification and differentiation in the adult mammalian intestine. *Nat. Rev. Mol. Cell Biol.* **22**, 39–53 (2021).

4. Ayabe, T. *et al.* Secretion of microbicidal α-defensins by intestinal Paneth cells in response to bacteria. *Nat. Immunol.* **1**, 113–118 (2000).

5. Nakamura, K. *et al.* Expression and Localization of Paneth Cells and Their α-Defensins in the Small Intestine of Adult Mouse. *Front. Immunol.* **11**, 570296 (2020).

6. Barker, N. *et al.* Identification of stem cells in small intestine and colon by marker gene Lgr5. *Nature* **449**, 1003–1007 (2007).

7. Sato, T. *et al.* Paneth cells constitute the niche for Lgr5 stem cells in intestinal crypts. *Nature* **469**, 415–418 (2011).

8. Pitman, R. S. & Blumberg, R. S. First line of defense: the role of the intestinal epithelium as an active component of the mucosal immune system. *J. Gastroenterol.* **35**, 805–814 (2000).

9. Bjerknes, M. & Cheng, H. [14] - Intestinal Epithelial Stem Cells and Progenitors. in *Methods in*

Enzymology (eds. Klimanskaya, I. & Lanza, R.) vol. 419 337–383 (Academic Press, 2006).

10. Sato, T. *et al.* Single Lgr5 stem cells build crypt-villus structures in vitro without a mesenchymal niche. *Nature* **459**, 262–265 (2009).

11. Han, X. *et al.* Creating a More Perfect Union: Modeling Intestinal Bacteria-Epithelial Interactions Using Organoids. *Cell Mol Gastroenterol Hepatol* **12**, 769–782 (2021).

12. Almeqdadi, M., Mana, M. D., Roper, J. & Yilmaz, Ö. H. Gut organoids: mini-tissues in culture to study intestinal physiology and disease. *Am. J. Physiol. Cell Physiol.* **317**, C405–C419 (2019).

13. Yin, Y.-B., de Jonge, H. R., Wu, X. & Yin, Y.-L. Mini-gut: a promising model for drug development. *Drug Discov. Today* **24**, 1784–1794 (2019).

14. Koo, B.-K. *et al.* Controlled gene expression in primary *Lgr5* organoid cultures. *Nat. Methods* **9**, 81–83 (2012).

15. Schwank, G., Andersson-Rolf, A., Koo, B.-K., Sasaki, N. & Clevers, H. Generation of BAC Transgenic Epithelial Organoids. *PLoS One* **8**, e76871 (2013).

16. Onuma, K. *et al.* Genetic reconstitution of tumorigenesis in primary intestinal cells. *Proc. Natl. Acad. Sci. U. S. A.* **110**, 11127–11132 (2013).

17. Fujii, M., Matano, M., Nanki, K. & Sato, T. Efficient genetic engineering of human intestinal organoids using electroporation. *Nat. Protoc.* **10**, 1474–1485 (2015).

18. Haber, A. L. *et al.* A single-cell survey of the small intestinal epithelium. *Nature* **551**, nature24489

(2017).

19. Yokoi, Y. *et al.* Paneth cell granule dynamics on secretory responses to bacterial stimuli in enteroids. *Sci. Rep.* **9**, 2710 (2019).

20. Yokoi, Y. *et al.* Simultaneous real-time analysis of Paneth cell and intestinal stem cell response to interferon-γ by a novel stem cell niche tracking method. *Biochem. Biophys. Res. Commun.* **545**, 14–19 (2021).

21. Eriguchi, Y. *et al.* Essential role of IFN-γ in T cell–associated intestinal inflammation. *JCI Insight* **3**, (2018).

22. Davis, H. E., Morgan, J. R. & Yarmush, M. L. Polybrene increases retrovirus gene transfer efficiency by enhancing receptor-independent virus adsorption on target cell membranes. *Biophys. Chem.* **97**, 159–172 (2002).

23. van der Flier, L. G., Haegebarth, A., Stange, D. E., van de Wetering, M. & Clevers, H. OLFM4 Is a Robust Marker for Stem Cells in Human Intestine and Marks a Subset of Colorectal Cancer Cells. *Gastroenterology* **137**, 15–17 (2009).

24. Takakuwa, A. *et al.* Butyric Acid and Leucine Induce α-Defensin Secretion from Small Intestinal Paneth Cells. *Nutrients* **11**, 2817 (2019).

25. Giblin, L. J. *et al.* Zinc-secreting Paneth cells studied by ZP fluorescence. *J. Histochem. Cytochem.* **54**, 311–316 (2006).

26. Barker, N., van Oudenaarden, A. & Clevers, H. Identifying the stem cell of the intestinal crypt: strategies and pitfalls. *Cell Stem Cell* **11**, 452–460 (2012).

27. Snippert, H. J. *et al.* Intestinal Crypt Homeostasis Results from Neutral Competition between Symmetrically Dividing Lgr5 Stem Cells. *Cell* **143**, 134–144 (2010).

28. Gehart, H. & Clevers, H. Tales from the crypt: new insights into intestinal stem cells. *Nat. Rev. Gastroenterol. Hepatol.* **16**, 19–34 (2019).

29. Van Lidth de Jeude, J. F., Vermeulen, J. L. M., Montenegro-Miranda, P. S., Van den Brink, G. R. & Heijmans, J. A Protocol for Lentiviral Transduction and Downstream Analysis of Intestinal Organoids. *J. Vis. Exp.* (2015) doi:10.3791/52531.

30. Kutner, R. H., Zhang, X.-Y. & Reiser, J. Production, concentration and titration of pseudotyped HIV-1-based lentiviral vectors. *Nat. Protoc.* **4**, 495–505 (2009).

31. Segura, M. M., Mangion, M., Gaillet, B. & Garnier, A. New developments in lentiviral vector design, production and purification. *Expert opinion on biological therapy* vol. 13 987–1011 Preprint at https://doi.org/10.1517/14712598.2013.779249 (2013).

32. Merten, O.-W., Hebben, M. & Bovolenta, C. Production of lentiviral vectors. *Molecular Therapy - Methods & Clinical Development* **3**, 16017 (2016).

33. Zietek, T. *et al.* Organoids to Study Intestinal Nutrient Transport, Drug Uptake and Metabolism - Update to the Human Model and Expansion of Applications. *Front Bioeng Biotechnol* **8**, 577656

(2020).

34. Mizutani, T. *et al.* Real-time analysis of P-glycoprotein-mediated drug transport across primary intestinal epithelium three-dimensionally cultured in vitro. *Biochem. Biophys. Res. Commun.* **419**, 238–243 (2012).

35. Zietek, T., Rath, E., Haller, D. & Daniel, H. Intestinal organoids for assessing nutrient transport, sensing and incretin secretion. *Sci. Rep.* **5**, 16831 (2015).

36. Kamioka, M. *et al.* Intestinal commensal microbiota and cytokines regulate Fut2+ Paneth cells for gut defense. *Proc. Natl. Acad. Sci. U. S. A.* **119**, (2022).

37. Shimizu, Y. *et al.* Paneth cell α-defensin misfolding correlates with dysbiosis and ileitis in Crohn's disease model mice. *Life Sci Alliance* **3**, (2020).

38. Buttó, L. F. *et al.* Intestinal Stem Cell Niche Defects Result in Impaired 3D Organoid Formation in Mouse Models of Crohn's Disease-like Ileitis. *Stem Cell Reports* **15**, 389–407 (2020).

39. Vidović, D. *et al.* rAAV-CFTRΔR Rescues the Cystic Fibrosis Phenotype in Human Intestinal Organoids and Cystic Fibrosis Mice. *Am. J. Respir. Crit. Care Med.* **193**, 288–298 (2016).

40. Montini, E. *et al.* Hematopoietic stem cell gene transfer in a tumor-prone mouse model uncovers low genotoxicity of lentiviral vector integration. *Nat. Biotechnol.* **24**, 687–696 (2006).

41. Montini, E. *et al.* The genotoxic potential of retroviral vectors is strongly modulated by vector design and integration site selection in a mouse model of HSC gene therapy. *J. Clin. Invest.* **119**,

964–975 (2009).

42. Yin, X. *et al.* Niche-independent high-purity cultures of Lgr5+ intestinal stem cells and their progeny. *Nat. Methods* **11**, 106–112 (2014).

43. Sato, T. *et al.* Long-term Expansion of Epithelial Organoids From Human Colon, Adenoma, Adenocarcinoma, and Barrett's Epithelium. *Gastroenterology* **141**, 1762–1772 (2011).

44. Denu, J. M. Vitamin B3 and sirtuin function. *Trends Biochem. Sci.* **30**, 479–483 (2005).

45. Saliba, A.-E., Westermann, A. J., Gorski, S. A. & Vogel, J. Single-cell RNA-seq: advances and future challenges. *Nucleic Acids Res.* **42**, 8845–8860 (2014).

46. Wang, F. *et al.* Isolation and Characterization of Intestinal Stem Cells Based on Surface Marker Combinations and Colony-Formation Assay. *Gastroenterology* **145**, 383-395.e21 (2013).

47. Gracz, A. D., Ramalingam, S. & Magness, S. T. Sox9 expression marks a subset of CD24-expressing small intestine epithelial stem cells that form organoids in vitro. *Am. J. Physiol. Gastrointest. Liver Physiol.* **298**, G590-600 (2010).

48. Farin, H. F. *et al.* Paneth cell extrusion and release of antimicrobial products is directly controlled by immune cell–derived IFN-γ. *J. Exp. Med.* **211**, 1393–1405 (2014).

49. Hayase, E. *et al.* R-Spondin1 expands Paneth cells and prevents dysbiosis induced by graft-versus-host disease. *J. Exp. Med.* jem.20170418 (2017) doi:10.1084/jem.20170418.

50. Wilson, C. L. *et al.* Regulation of intestinal alpha-defensin activation by the metalloproteinase

matrilysin in innate host defense. *Science* **286**, 113–117 (1999).

51. Salzman, N. H. *et al.* Enteric defensins are essential regulators of intestinal microbial ecology. *Nat. Immunol.* **11**, 76 (2010).

52. Masuda, K., Sakai, N., Nakamura, K., Yoshioka, S. & Ayabe, T. Bactericidal Activity of Mouse α-Defensin Cryptdin-4 Predominantly Affects Noncommensal Bacteria. *J. Innate Immun.* **3**, 315–326 (2011).

53. Eriguchi, Y. *et al.* Graft-versus-host disease disrupts intestinal microbial ecology by inhibiting Paneth cell production of α-defensins. *Blood* **120**, 223–231 (2012).

54. Eriguchi, Y. *et al.* Decreased secretion of Paneth cell α-defensins in graft-versus-host disease. *Transpl. Infect. Dis.* **17**, 702–706 (2015).

55. Nakamura, K., Sakuragi, N. & Ayabe, T. A monoclonal antibody-based sandwich enzyme-linked immunosorbent assay for detection of secreted α-defensin. *Anal. Biochem.* **443**, 124–131 (2013).

56. Suzuki, K. *et al.* Decrease of α-defensin impairs intestinal metabolite homeostasis via dysbiosis in mouse chronic social defeat stress model. *Sci. Rep.* **11**, 1–15 (2021).

57. Satoh, Y., Habara, Y., Ono, K. & Kanno, T. Carbamylcholine- and catecholamine-induced intracellular calcium dynamics of epithelial cells in mouse ileal crypts. *Gastroenterology* **108**, 1345–1356 (1995).

58. Yang, J. & Yan, H. TLR5: beyond the recognition of flagellin. *Cell. Mol. Immunol.* **14**, 1017–

1019 (2017).

59. Brackett, C. M. *et al.* Signaling through TLR5 mitigates lethal radiation damage by neutrophil-dependent release of MMP-9. *Cell Death Discov* **7**, 266 (2021).

60. Knoop, K. A., McDonald, K. G., McCrate, S., McDole, J. R. & Newberry, R. D. Microbial sensing by goblet cells controls immune surveillance of luminal antigens in the colon. *Mucosal Immunol.* **8**, 198–210 (2015).

61. Gustafsson, J. K. & Johansson, M. E. V. The role of goblet cells and mucus in intestinal homeostasis. *Nat. Rev. Gastroenterol. Hepatol.* **19**, 785–803 (2022).

62. Tanabe, H. *et al.* Mouse paneth cell secretory responses to cell surface glycolipids of virulent and attenuated pathogenic bacteria. *Infect. Immun.* **73**, 2312–2320 (2005).

63. Silva, P. N., Altamentova, S. M., Kilkenny, D. M. & Rocheleau, J. V. Fibroblast Growth Factor Receptor Like-1 (FGFRL1) Interacts with SHP-1 Phosphatase at Insulin Secretory Granules and Induces Beta-cell ERK1/2 Protein Activation*. *J. Biol. Chem.* **288**, 17859–17870 (2013).

64. Lawrence, M., Shao, C., Duan, L., McGlynn, K. & Cobb, M. H. The protein kinases ERK1/2 and their roles in pancreatic beta cells. *Acta Physiol.* **192**, 11–17 (2008).

65. Zheng, Y. *et al.* Interleukin-22 mediates early host defense against attaching and effacing bacterial pathogens. *Nat. Med.* **14**, 282−289 (2008).

66. Zenewicz, L. A. *et al.* Innate and adaptive interleukin-22 protects mice from inflammatory bowel

disease. *Immunity* **29**, 947–957 (2008).

67. Gaudino, S. J. *et al.* IL-22 receptor signaling in Paneth cells is critical for their maturation, microbiota colonization, Th17-related immune responses, and anti-Salmonella immunity. *Mucosal Immunol.* **14**, 389–401 (2021).

68. Zerial, M. & McBride, H. Rab proteins as membrane organizers. *Nat. Rev. Mol. Cell Biol.* **2**, 107–117 (2001).

69. Pombo, I. *et al.* IgE Receptor Type I-dependent Regulation of a Rab3D-associated Kinase: A POSSIBLE LINK IN THE CALCIUM-DEPENDENT ASSEMBLY OF SNARE COMPLEXES*. *J. Biol. Chem.* **276**, 42893–42900 (2001).

70. Ohnishi, H., Samuelson, L. C., Yule, D. I., Ernst, S. A. & Williams, J. A. Overexpression of Rab3D enhances regulated amylase secretion from pancreatic acini of transgenic mice. *J. Clin. Invest.* **100**, 3044–3052 (1997).

71. Pastor-Cantizano, N., Montesinos, J. C., Bernat-Silvestre, C., Marcote, M. J. & Aniento, F. p24 family proteins: key players in the regulation of trafficking along the secretory pathway. *Protoplasma* **253**, 967–985 (2016).

72. Zhang, M. *et al.* A Translocation Pathway for Vesicle-Mediated Unconventional Protein Secretion. *Cell* **181**, 637-652.e15 (2020).

73. Wang, C.-C. *et al.* A role of VAMP8/endobrevin in regulated exocytosis of pancreatic acinar cells.

Dev. Cell **7**, 359–371 (2004).

74. Jones, L. C. *et al.* VAMP8 is a vesicle SNARE that regulates mucin secretion in airway goblet cells. *J. Physiol.* **590**, 545–562 (2012).

75. Zhao, C., Slevin, J. T. & Whiteheart, S. W. Cellular functions of NSF: not just SNAPs and SNAREs. *FEBS Lett.* **581**, 2140–2149 (2007).

76. Xu, T., Ashery, U., Burgoyne, R. D. & Neher, E. Early requirement for alpha-SNAP and NSF in the secretory cascade in chromaffin cells. *EMBO J.* **18**, 3293–3304 (1999).

7. Figures

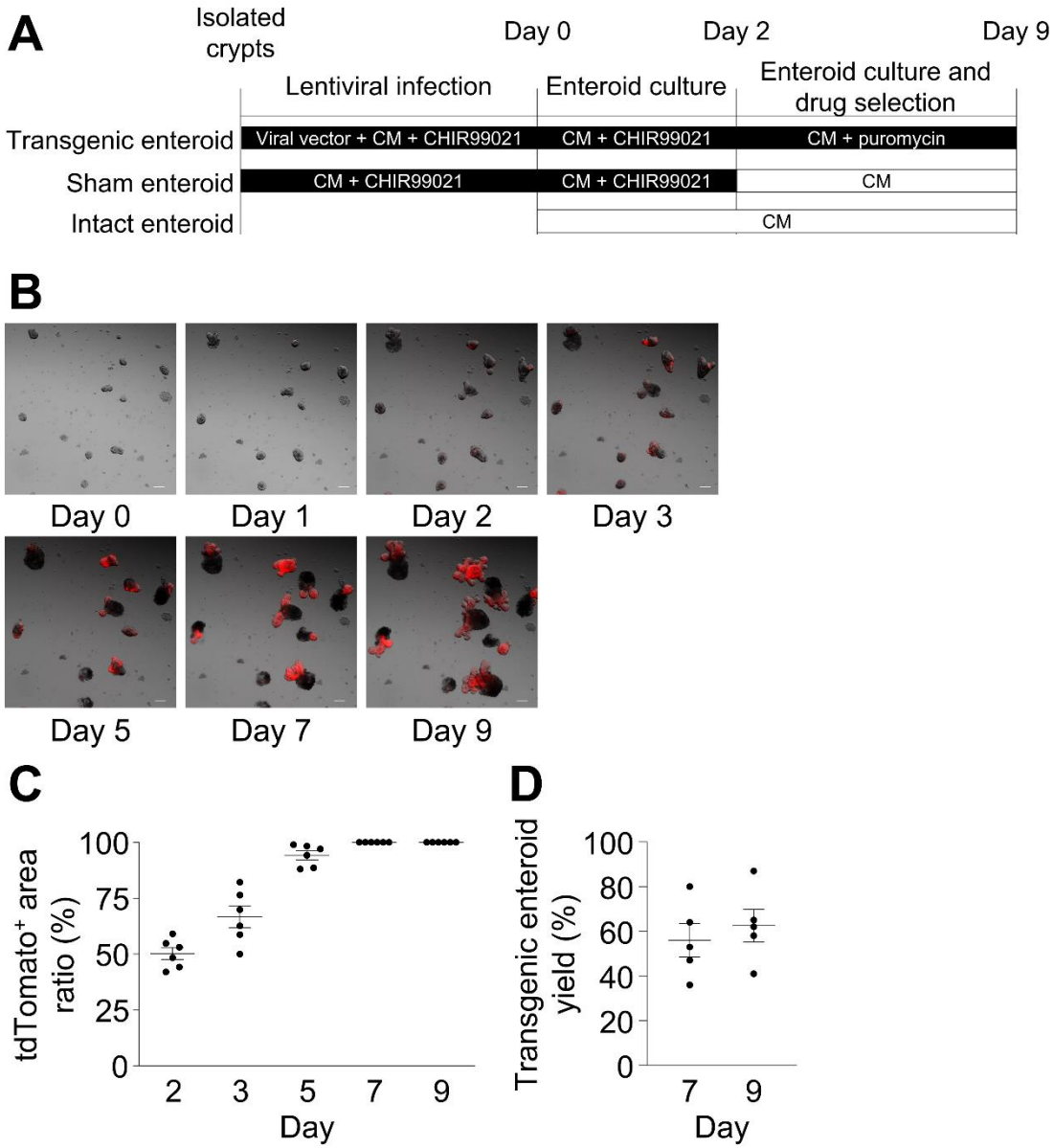

Figure 1. Formation of transgenic enteroids by gene transfer into isolated crypts

(A) Schematic process of gene transfer, culture, and drug selection. (B) Growth of isolated crypts transferred tdTomato (red). Scale bars: 100 μm. (C) TdTomato^{+} area ratio in enteroids during culture. (D) The yield of obtained transgenic enteroids at day 7 and 9. The assays were performed in six (C)

and five (D) independent experiments. Data are mean ± SEM. No significant changes were observed, Student's t-test.

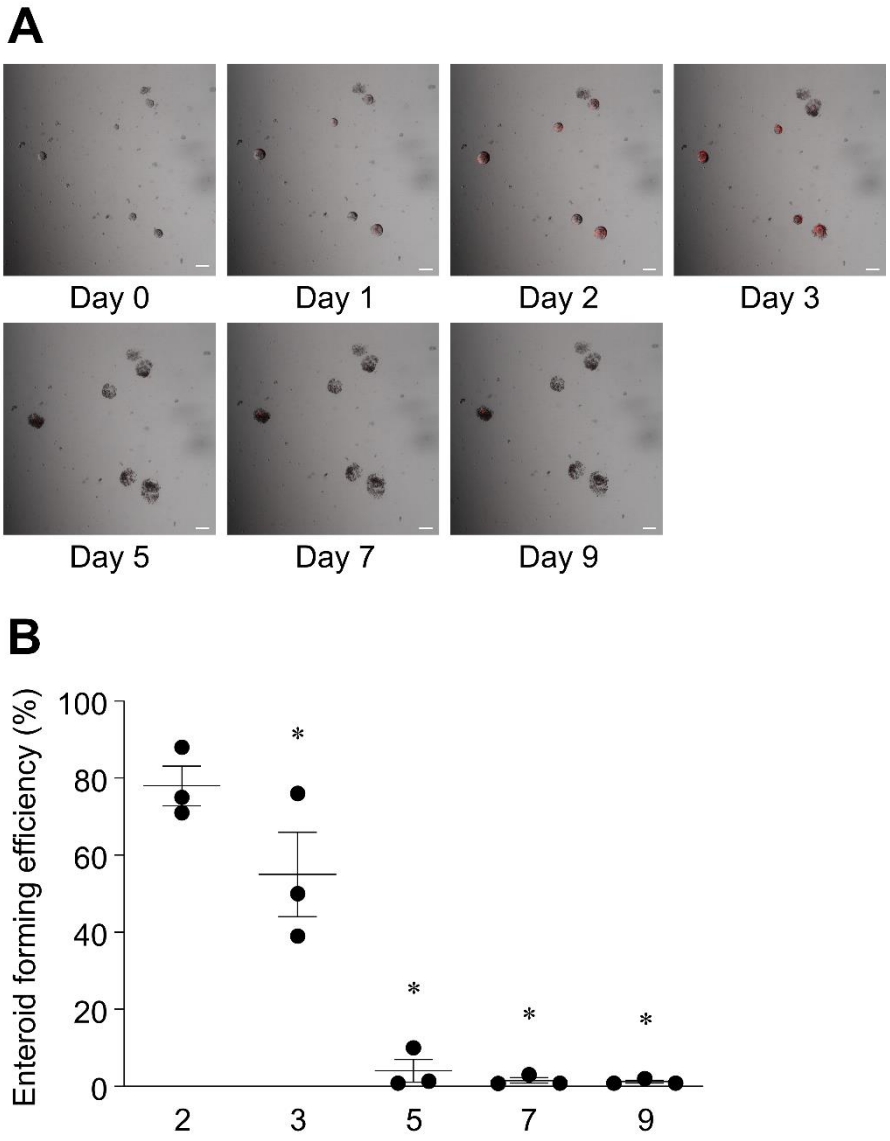

Figure 2. Disruption of transgenic enteroids by adding polybrene during gene transfer

(A) Growth of isolated crypts transferred tdTomato (red) with polybrene. Scale bar: 100 μm. (B) Forming efficiency of enteroids generated from isolated crypts transferred with polybrene. Day 2: 78 ± 5.1%; Day 3: 55 ± 11%; Day 5: 4.1 ± 2.9%; Day 7: 1.6 ± 0.75%; Day 9: 1.4 ± 0.53%. The assays were performed in three independent experiments. Data are mean ± SEM. *$P < 0.05$, one-way ANOVA with Dunnett's post hoc test compared with day 2.

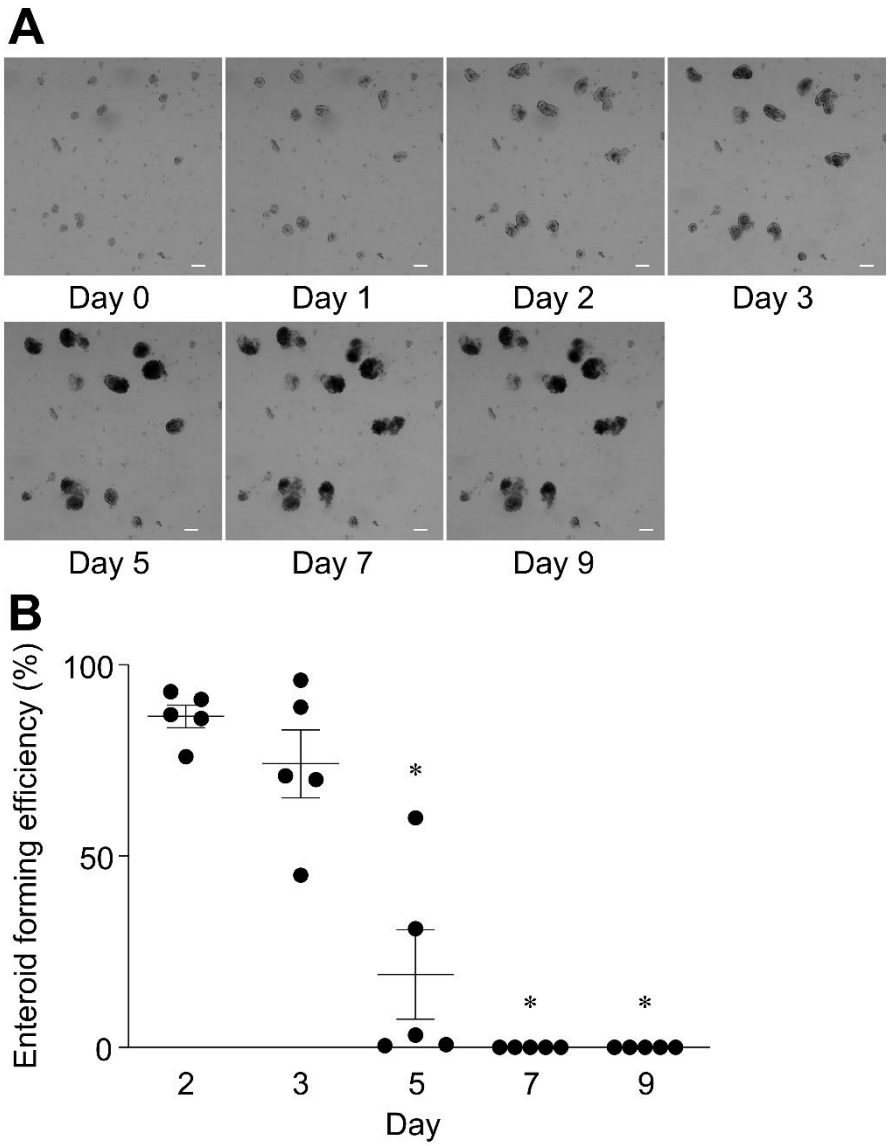

Figure 3. Examination of drug selection condition

(A) Representative images of intact enteroids that were not transferred puromycin-resistant gene and treated with 2 μg/mL puromycin after day 2. Scale bar: 100 μm. (B) Forming efficiency of intact enteroids treated with 2 μg/mL puromycin. Day 2: 87 ± 2.9%; Day 3: 74 ± 8.8%; Day 5: 19 ± 12%; Day 7: 0.0 ± 0.0%; Day 9: 0.0 ± 0.0%. The assays were performed in five independent experiments.

Data are mean ± SEM. *P < 0.05, one-way ANOVA with Dunnett's post hoc test compared with day 2.

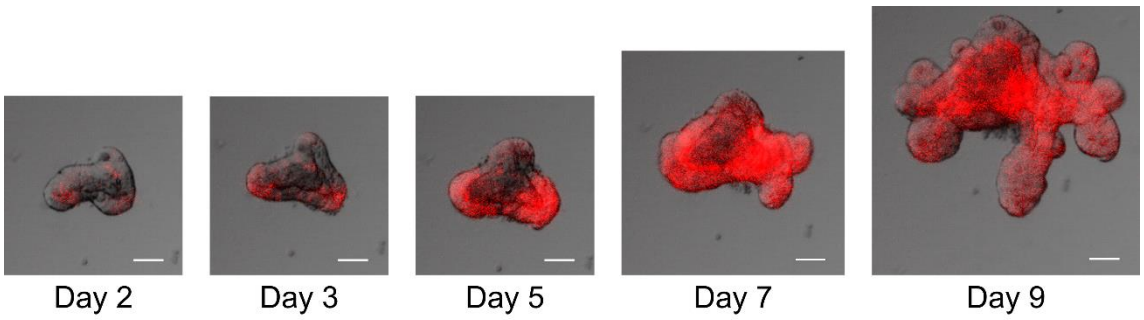

Figure 4. Process of transgenic enteroid formation

Representative images of formation process for transgenic enteroid. TdTomato (red) was shown. Scale bars: 50 μm.

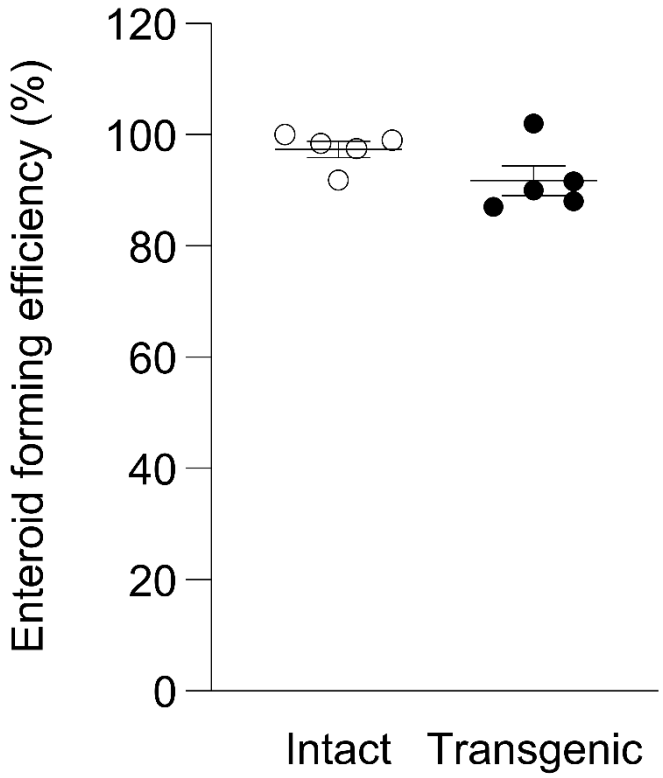

Figure 5. Effect of gene transfer manipulation on enteroid formation

Forming efficiency of intact and transgenic enteroid at day 2. Intact: 97 ± 1.4%, transgenic: 92 ± 2.7%. The assays were performed in five independent experiments. Data are mean ± SEM. No significant changes were observed, Student's t-test.

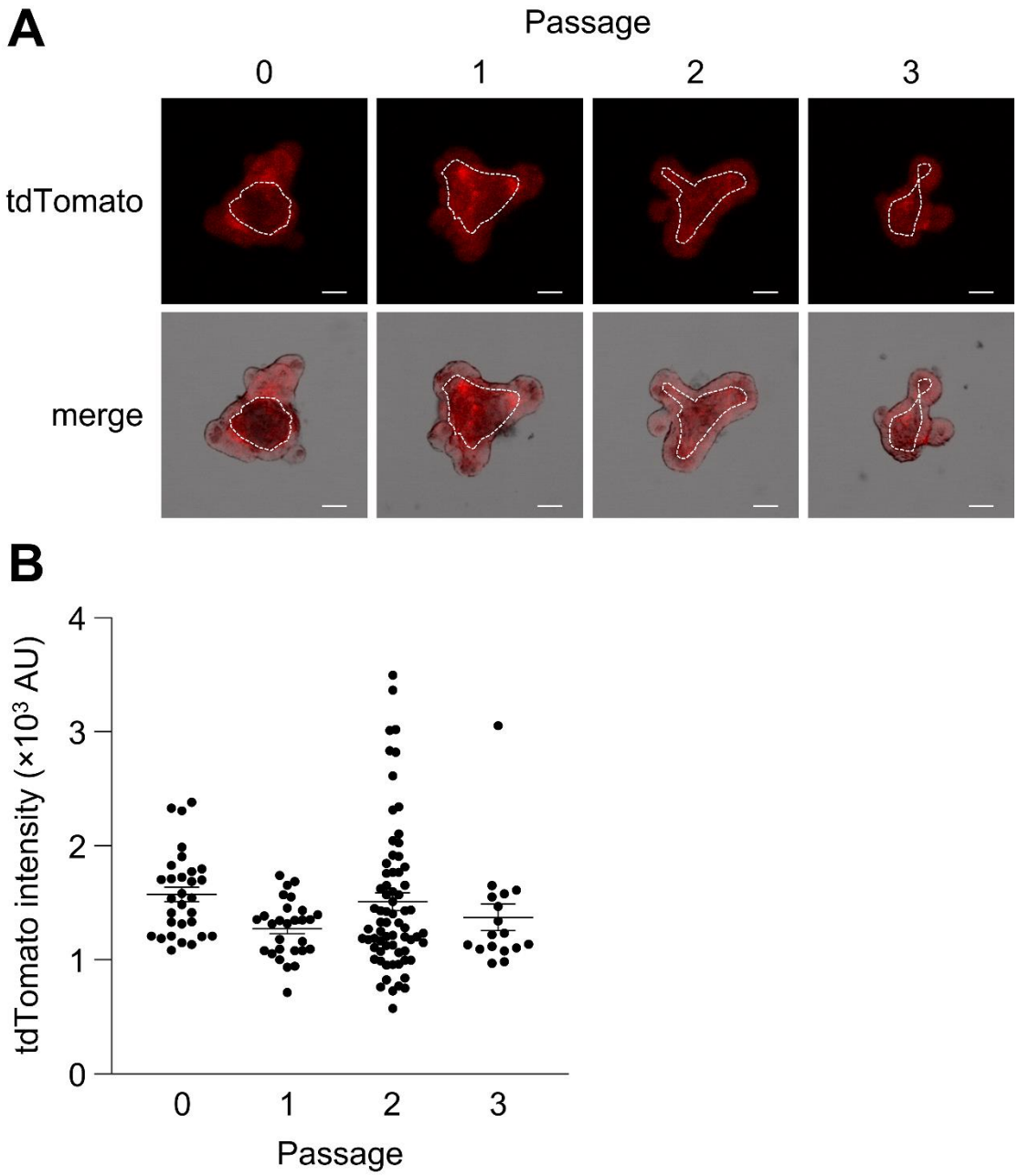

Figure 6. Maintenance of transgene expression in transgenic enteroid during passage culture

(A) Representative images of the transgenic enteroid at each passages. The dotted line outlines the central lumen with autofluorescence. tdTomato (red) was shown. Scale bar: 50 μm. (B) Transgene expression of transgenic enteroid during passage culture. The assays were performed in 18–83

enteroids. Data are mean ± SEM. No significant changes were observed, One-way ANOVA with Dunnett's post hoc test compared with passage 0.

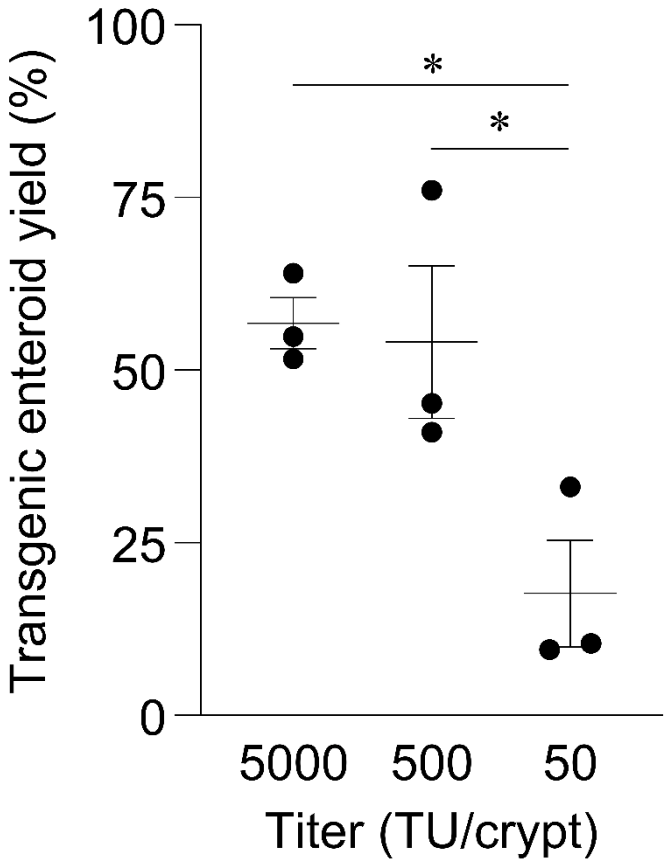

Figure 7. Effect of viral titer on formation of transgenic enteroid

The yield of transgenic enteroids produced from isolated crypts transduced with 5.0×10^3, 5.0×10^2 and 5.0×10 TU / crypt lentiviral vectors. The assays were performed in three independent experiments. Data are mean ± SEM. *P < 0.05, one-way ANOVA with Tukey's post hoc test.

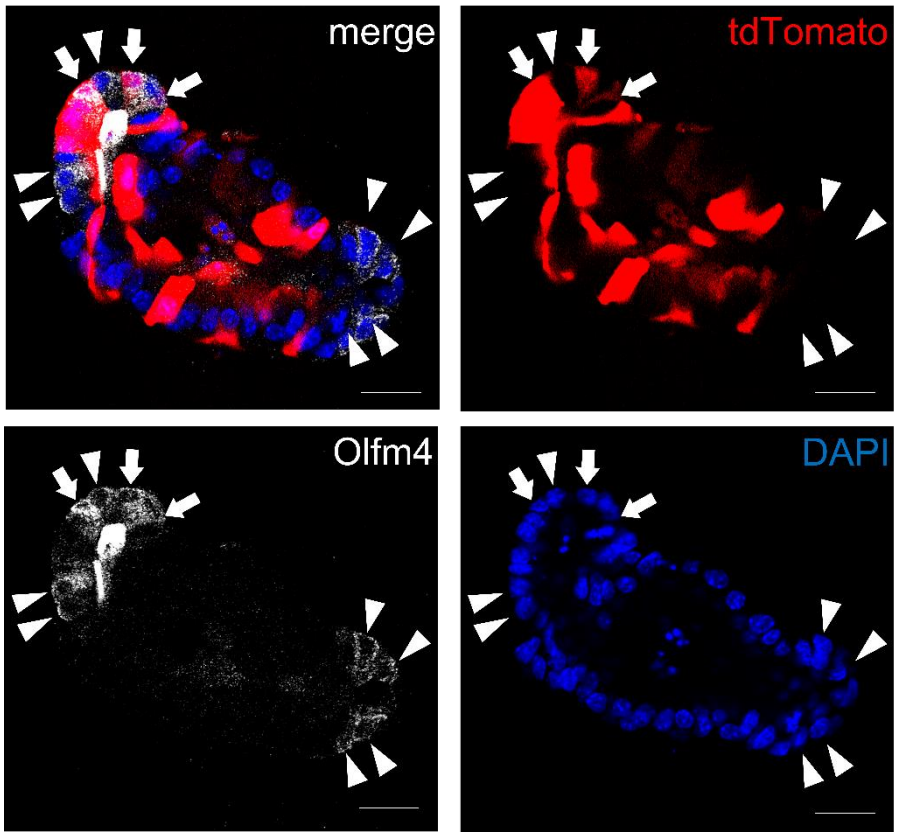

Figure 8. Transgenic enteroid generation by gene transferred intestinal epithelial stem cells

Representative immunofluorescence images of Olfm4 (white) in transgenic enteroids expressing tdTomato (red) at day 2. Nuclei (Blue), $tdTomato^{+}Olfm4^{+}$ cell (white arrow), $tdTomato^{-}Olfm4^{+}$ cell (white arrowhead) were shown. Scale bars: 20 μm.

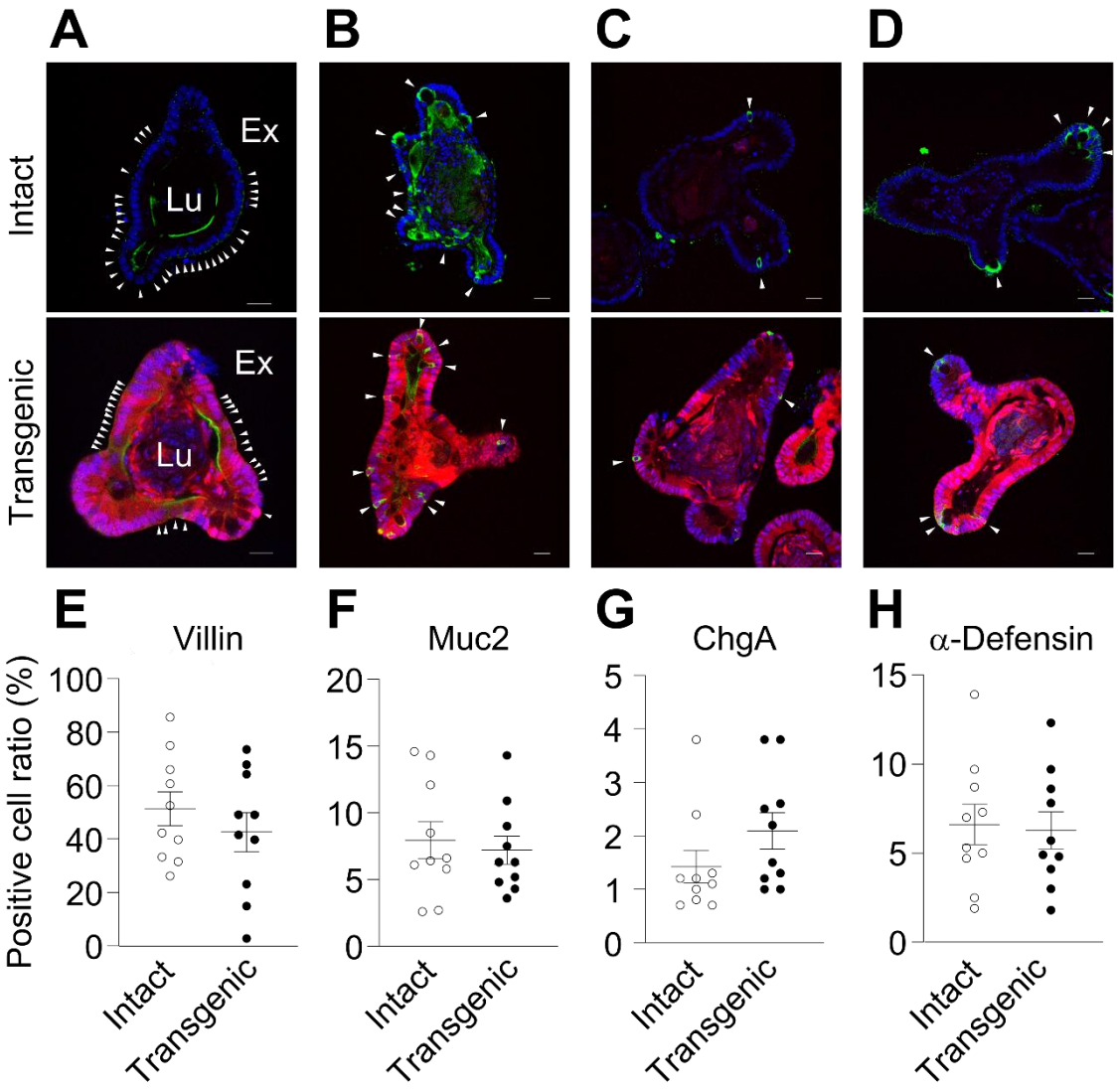

Figure 9. Maintenance of multipotency in gene transferred intestinal epithelial stem cells

(A–D) Representative immunofluorescence images of transgenic enteroid at day 7 with villin (A, green), Muc2 (B, green), ChgA (C, green), or α-defensin (D, green). Each marker-expressing cell was indicated by white arrowheads. TdTomato (red), nuclei (Blue), the lumen (Lu), and the exterior (Ex) were shown. Scale bar 20 μm. (E–H) The ratio of villin$^+$ (E), Muc2$^+$ (F), ChgA$^+$ (G), or α-defensin$^+$

(H) cells in intact and transgenic enteroids. The assays were performed in 10 enteroids. Data are mean ± SEM. No significant changes were observed, Student's t-test.

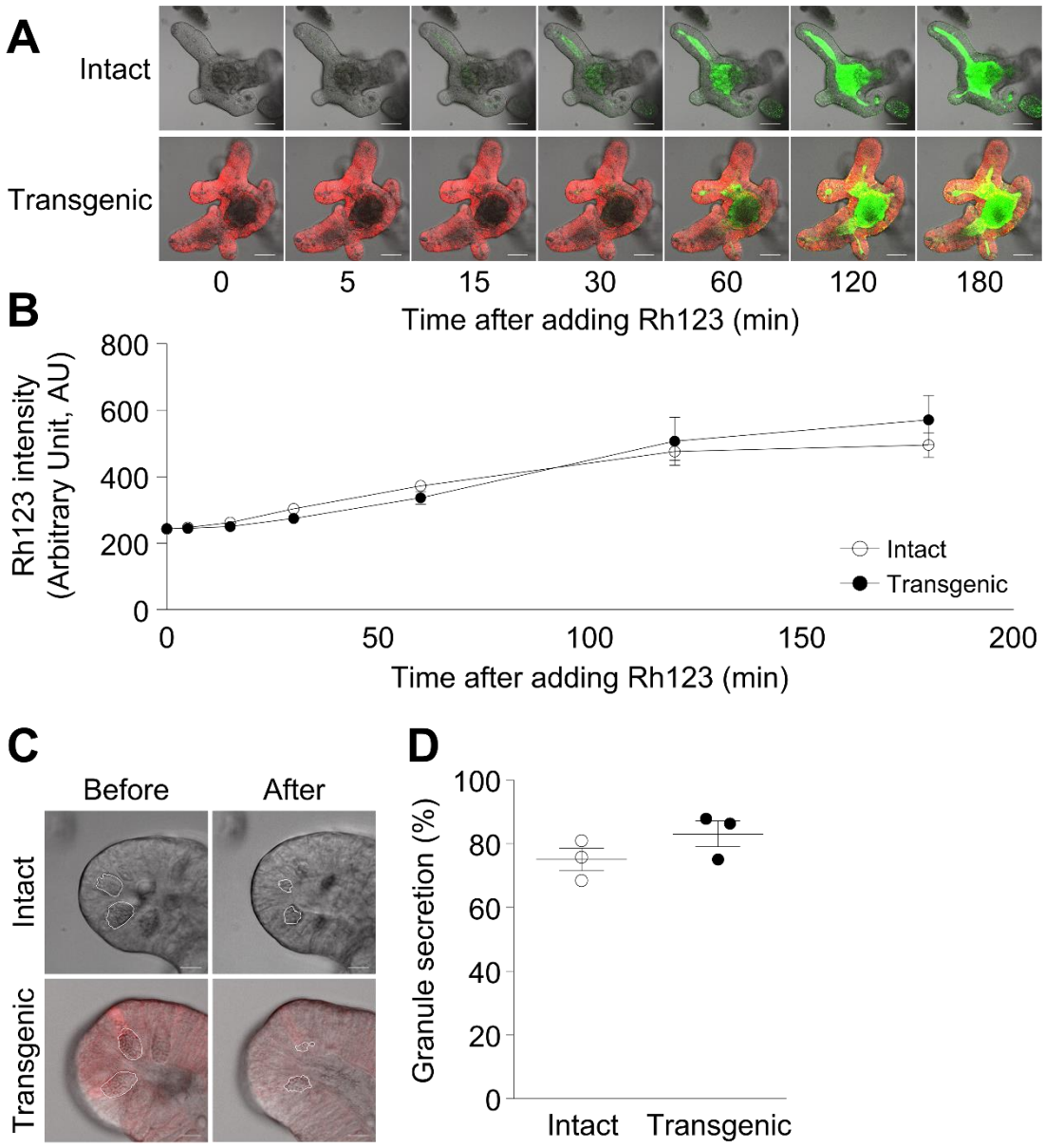

Figure 10. Maintenance of function in terminally differentiated cells derived from gene transferred intestinal epithelial stem cells

(A) Representative fluorescence and DIC images of intact and transgenic enteroids 0, 5, 15, 30, 60, 120, and 180 min after adding Rh123 (green). TdTomato (red) was shown. Scale bar: 50 μm. (B) Rh123 intensity in the lumen of intact (open circle) and transgenic (closed circle) enteroids. No

significant changes were observed between intact and transgenic enteroid at all time points, Two-way ANOVA with Bonferroni's post hoc test. (C) Representative images of Paneth cell granules (white line) in the intact and transgenic enteroid before and after adding CCh. TdTomato (red) was shown. Scale bar: 10 μm. (D) Percent granule secretion of Paneth cells in intact and transgenic enteroids 30 min after adding CCh. The assays were performed in three independent experiments. Data are mean ± SEM. No significant changes were observed, Student's t-test.

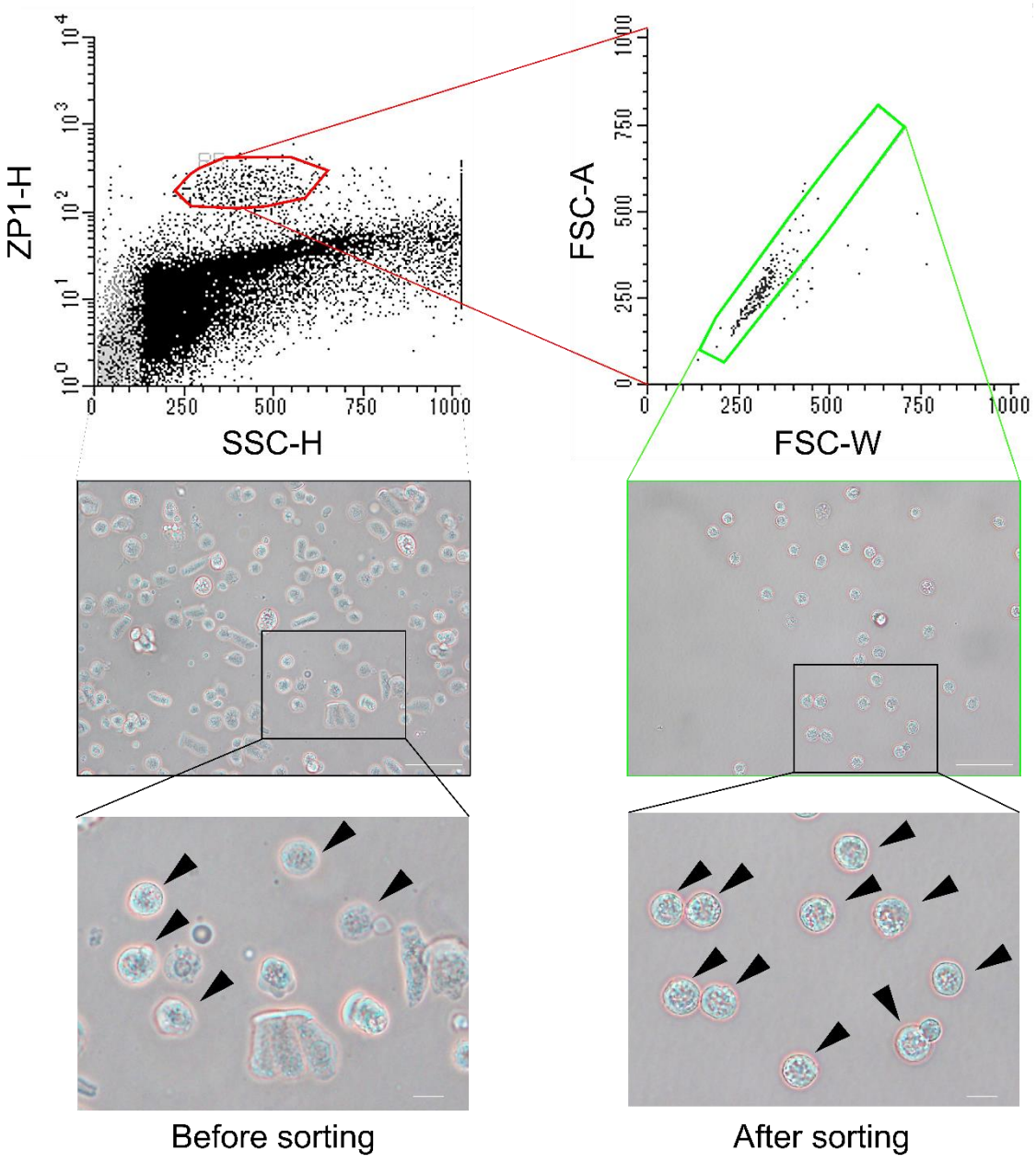

Figure 11. Isolation of Paneth cells by FACS

FACS gating strategy and the representative image of sorted cell populations. Paneth cells were shown in arrowheads. Scale bar: 50 μm (low magnification), 10 μm (high magnification).

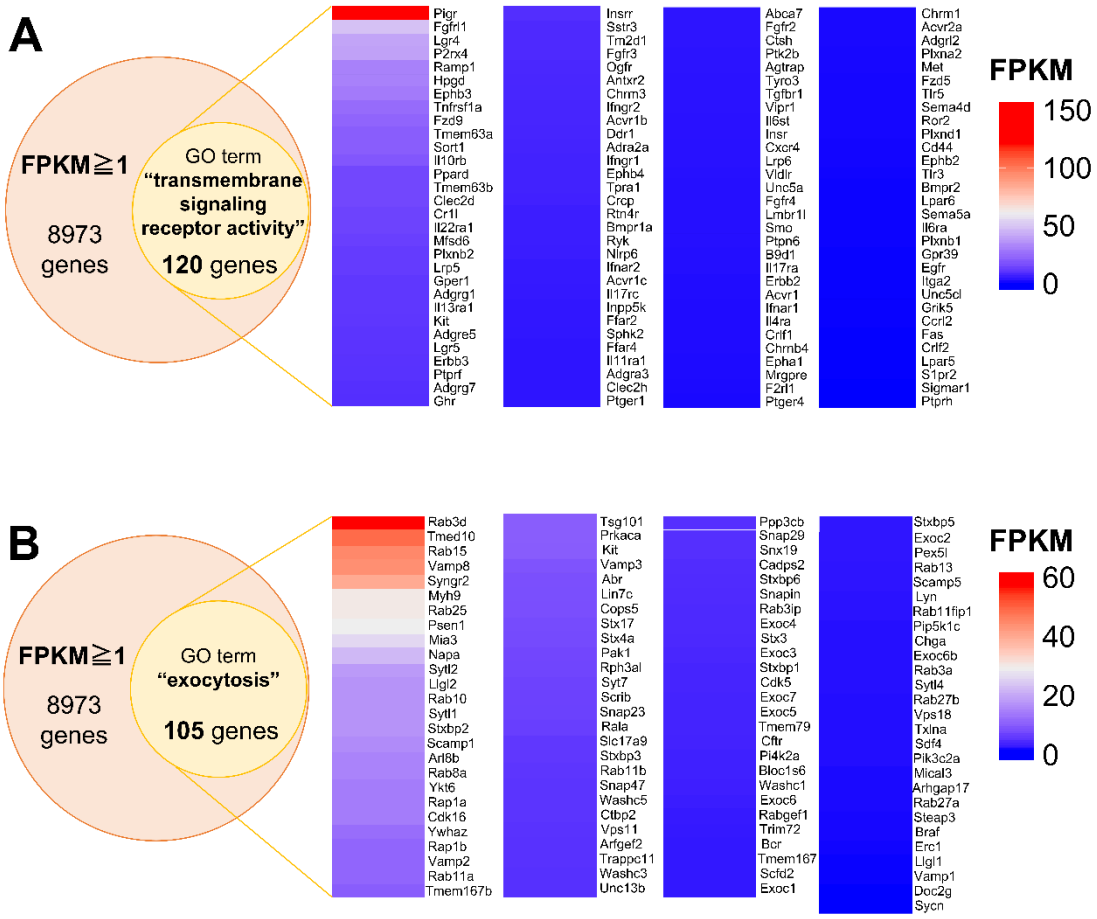

Figure 12. Functional genes identified in Paneth cells.

(A, B) Sorted Paneth cells were analyzed by RNA-seq. Genes annotated with GO term "transmembrane signaling receptor activity" (A) and "exocytosis" (B) were shown.

8. Acknowledgements

First, I would like to express my deep gratitude to my supervisor, Associate Professor Kiminori Nakamura. He always gives me prompt guidance, scientific ideas, and valuable suggestions throughout my doctoral study. I also would like to show my grateful appreciation to Professor Tokiyoshi Ayabe. I could keep going my doctoral study with his sincere encouragement and excellent guidance. I gratefully appreciate to Professor Tomoyasu Aizawa and Professor Hisashi Haga for continuing support and valuable advice. I thank Assistant Professor Yuki Yokoi in the Innate Immunity Laboratory for enormous technical support and helpful advice. I would like to thank Dr. Yu Shimizu, Ms. Aiko Kuroishi and Ms. Atsuko Shibanuma for technical help and useful discussion. I am deeply grateful to Ms. Mari Tatsumi. She always supports my laboratory activities. Finally, I want to thank all laboratory members for continuing support for my laboratory life.

I appreciate the financial support from Research Fellowships of Japan Society for the Promotion of Science (JSPS) for Young Scientists and Hokkaido University DX doctoral fellowship. This study was supported by JSPS KAKENHI Grant Number 22J10521 and Hokkaido University DX doctoral fellowship Grant Number JPMJSP2119.